8th Biennial International Conference
& Exposition on Petroleum Geophysics

"HYDERABAD 2010"

P-09

AVO Techniques: Advantages, Limitations and Future Prospects

Deepak Singh, *ISM, Dhanbad*

Summary

Amplitude versus offset

In geophysics, ***amplitude versus offset*** *(AVO) or* ***amplitude variation with offset*** *is a variation in seismic reflection amplitude with change in distance between shot point and receiver. It is also referred as AVA (amplitude variation with angle). As AVO studies are being done on CMP data, the offset increases with the angle.*

An AVO anomaly is most commonly expressed as increasing (rising) AVO in a sedimentary section, often where the hydrocarbon reservoir is "softer" (lower acoustic impedance) than the surrounding shales. Typically amplitude decreases (falls) with offset due to geometrical spreading, attenuation and other factors. An AVO anomaly can also include examples where amplitude with offset falls at a lower rate than the surrounding reflective events.

Applications in the oil and gas industry

The most important application of AVO is the detection of hydrocarbon reservoirs. Rising AVO is typically pronounced in oil-bearing sediments, and even more so in gas-bearing sediments. Particularly important examples are those seen in deepwater turbidite sands such as the Late Tertiary deltaic sediments in the Gulf of Mexico (especially during the 1980s-1990s), West Africa, and other major deltas around the world. Most major companies use AVO routinely as a tool to "de-risk" exploration targets and to better define the extent and the composition of existing hydrocarbon reservoirs.

AVO is not fail-safe

An important caveat is that the existence of abnormally rising or falling amplitudes can sometimes be caused by other factors, such as alternative lithologies and residual hydrocarbons in a breached gas column. Not all oil and gas fields are associated with an obvious AVO anomaly (e.g. most of the oil found in the Gulf of Mexico in the last decade), and AVO analysis is by no means a panacea for gas and oil exploration.

Variation in seismic reflection amplitude with change in distance between shotpoint and receiver that indicates differences in lithology and fluid content in rocks above and below the reflector. AVO analysis is a technique by which geophysicists attempt to determine thickness, porosity, density, velocity, lithology and fluid content of rocks. Successful AVO analysis requires special processing of seismic data and seismic modeling to determine rock properties with a known fluid content. With that knowledge, it is possible to model other types of fluid content. A gas-filled sandstone might show increasing amplitude with offset, whereas a coal might show decreasing amplitude with offset. A limitation of AVO analysis using only P-energy is its failure to yield a unique solution, so AVO results are prone to misinterpretation. One common misinterpretation is the failure to distinguish a gas-filled reservoir from a reservoir having only partial

gas saturation ("fizz water"). However, AVO analysis using source-generated or mode-converted shear wave energy allows differentiation of degrees of gas saturation. AVO analysis is more successful in young, poorly consolidated rocks, such as those in the Gulf of Mexico, than in older, well-cemented sediments. than in older, well-cemented sediments.

Amplitude versus offset

As important as the relative response between different reflections is the amplitude response of a single reflection as a function of the offset, or the illumination angle. The two P-to-P reflections of the previous subsection are separately analyzed here. To allow a direct comparison with the analytical curve for the PP plane-wave reflection coefficient, the wavefields simulated by each of the methods were mapped to the *tau-p* domain, which corresponds to the plane-wave decomposition of the original wavefields. Each figure used in this analysis contains five curves. The two continuous curves correspond to the real and imaginary parts of the theoretical P-to-P *plane-wave response* as a function of the horizontal slowness. The theoretical response includes the PP reflection coefficient and the two-way (angle-dependent) PP transmission coefficient. The other three curves come from the tau-p transform of the simulated wavefields, multiplied by a scaling factor that normalizes the amplitudes of the fifteenth horizontal slowness to the theoretical amplitude.

Figure shows the curves associated with the water-bottom reflection. In the low horizontal slowness region the dual-operator curve (dashed-line) fits the theoretical curve almost perfectly, while the other two curves also represent a good approximation to the theoretical curve. It is also important to notice that the curve from the traditional finite-difference modeling (dashed-dotted-line) oscillates more than the other two curves. In the high horizontal slowness region, the traditional finite-difference method completely fails to approximate the theoretical curve while the other two methods still maintain a reasonably close fitting of the theoretical curve. One reason for the larger misfit here is the strong interference from the reflection of the second interface in the far offsets.

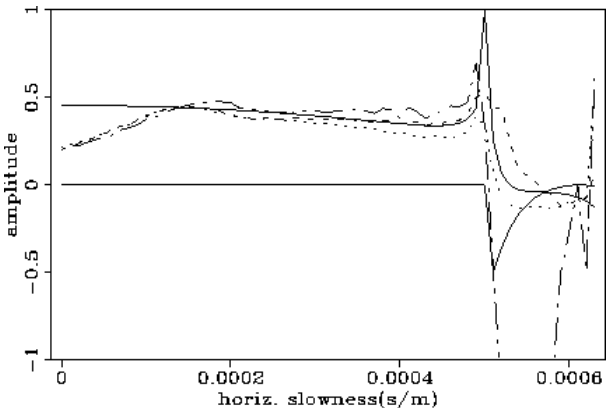

Figure 1 Amplitude versus horizontal slowness of the PP reflection from the water-bottom interface. These curves were extracted from the plane-wave decomposition of the wavefields generated by the three modeling schemes. The thick continuous line and the thin continuous line correspond, respectively, to the real and imaginary parts of the theoretical PP plane-wave reflection coefficient; the dotted-line is the amplitude response from the propagator-matrix scheme; the dashed-line is the amplitude response from the dual-operator scheme; the thin dot-dashed-line comes from the traditional finite-difference scheme.

As in the previous case, the curves for the second PP primary reflection (Figure 2) approximate well the theoretical curve for low values of horizontal slowness. Again, the curve from the traditional finite-difference scheme is much more jagged than the curves from the other two schemes. For larger values of horizontal slowness, the dual-operator and the propagator-matrix curves are closer to the theoretical curve than the traditional finite-difference curve with better fit than in the water bottom case, mainly because the interference from other events is much weaker in this case. Particularly impressive is the extremely good fit obtained by the dual-operator method (dashed-line) for the whole range of horizontal slownesses, including the

almost perfect prediction of the important zero-crossing point.

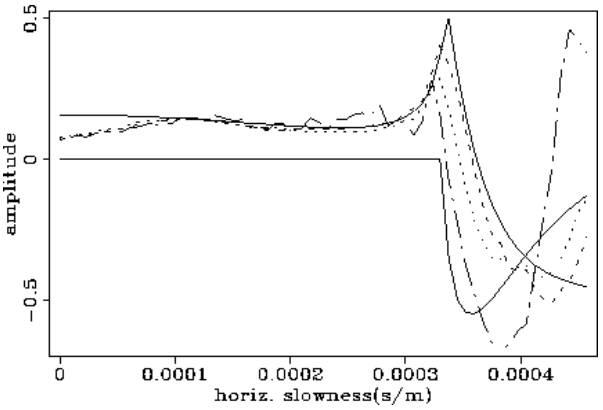

Figure 2 Amplitude versus horizontal slowness of the PP reflection from the interface between the second and third layer of the model. These curves were extracted from the plane-wave decomposition of the wavefields generated by the three modeling schemes. The thick continuous line and the thin continuous line correspond, respectively, to the real and imaginary parts of the theoretical PP plane-wave reflection coefficient; the dotted-line is the amplitude response from the propagator-matrix scheme; the dashed-line is the amplitude response from the dual-operator scheme; the thin dot-dashed-line comes from the traditional finite-difference scheme.

The zero-offset waveform

The first comparison involves the zero-offset response of the three methods. A window that includes the first two primary reflections (both PP) was selected from the zero-offset trace of the vertical components for the three simulated wavefields. Figure 3 shows the three waveforms. Except for small differences in the amplitude and the precursor lobe, the waveforms generated by the propagator-matrix and dual-operator methods are very similar. The dispersion is minimal and the kinematics are in accordance with theoretical expectations. The dispersive character observed in the wavefield of the traditional finite-difference scheme becomes more clear in the selected window. As a result of the dispersion, the traveltime difference between the two reflections (using the central picks as the measuring criterion) is slightly larger than the theoretical value.

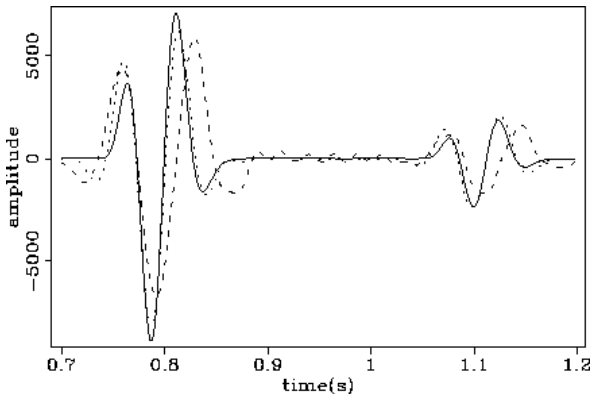

Figure 3 Zero offset response generated by the three schemes. The three curves correspond to a window selected from the first traces of Figures -a, -a, and -a, which include the reflections from the first two interfaces of the model. The continuous line comes from the Haskell-Thomson scheme, the dotted-line comes from the dual-operator scheme, and the dashed-line comes from the traditional finite-difference scheme.

The theoretical ratio between the amplitudes of the two reflections is given by

$$\frac{\mathrm{Amp}_2}{\mathrm{Amp}_1} = \frac{R_2}{R_1}\left(1 - R_1^2\right)\left[\frac{t_1 v_1^2}{(t_2 - t_1)v_2^2 + t_1 v_1^2}\right]^{1/2},$$

where the first term is the ratio between the normal incidence reflection coefficients, the second term is the two-way transmission coefficient, and the third term is the 2D-divergence relative correction. The value obtained from the propagator-matrix trace coincides with the predicted value, while the value from the dual-operator trace is 3.7 percent higher, and the value from the traditional finite-difference trace is 7.5 percent lower.